COMPUTATIONAL ANALYSIS OF A NEAR AND FAR SIDE FRONT OCCUPANT KINEMATICS IN A VEHICLE ROLLOVER WITH DIFFERENT RESTRAINTS

Chandrashekhar K. Thorbole
David A. Renfroe
Stephen A. Batzer
David Beltran
Grant Herndon
The Engineering Institute, LLC.
United States
Paper Number 09-0491

ABSTRACT

The Volvo XC 70 2001 model is used to conduct the full scale rollover crash test to determine the glazing and roof performance. The biodynamic code MADYMO is used to model the vehicle and its occupant. The acceleration obtained from the full scale rollover test is used to prescribe the motion to the computational model. The front side occupants are 50th percentile Hybrid III ATD's.

A Finite Element belt model is used for the analysis because of its capability to simulate the slip of the occupant under the shoulder belt. The simulation is carried out with different restraint types to quantify the head lateral and vertical excursions. The restraint type includes the conventional three-point system, integrated restraint in which the belt is attached to the seat, and a restraint type in which an extra shoulder belt is added to a conventional and an integrated restraint. The driver and the passenger head kinematics are compared for each restraint type. A comparasion is made for driver and passenger head excursion for different restraint types to demonstrate the effectiveness of each restraint in reducing excursion. The study indicates that an integrated seat belt results in less lateral and vertical head excursion, as compared to the conventional restraint. This study also indicates no significant improvement in reducing head excursion by the addition of an extra shoulder belt compared to a conventional or an integrated restraint.

INTRODUCTION

Seat belts are an important active safety device in a passenger vehicle. Seat belts are intended to reduce injuries to a passenger by preventing the passenger from hitting the interior due to declarative forces. It is estimated that seat belts are responsible for saving 147,246 lives in the period 1975-2001[1]. The lap and shoulder single continuous loop restraint is the most popular seat belt system in the passenger vehicle. This restraint performance is enhanced by the introduction of retractors, webbing grabber, load limiter and pre-tensioners. Three-point restraints play a crucial role in frontal impact by avoiding the secondary impact between the passenger and the vehicle interior. The effectiveness of this restraint during rollover depends on the roof integrity, as the intrusion of the B-pillar tends to move the D-ring generating the slack in the continuous belt loop [2]. The slack in the belt could result in partial or complete ejection causing fatal head and neck injury. Figure 1 shows the fatal complete/partial ejection from different vehicle types. Figure 2 shows the rollover occurrence by vehicle types, which indicates higher rollover propensity for utility vehicles [3].

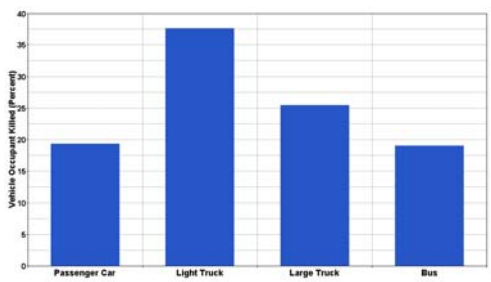

Figure 1. Fatal ejection from different vehicle types.

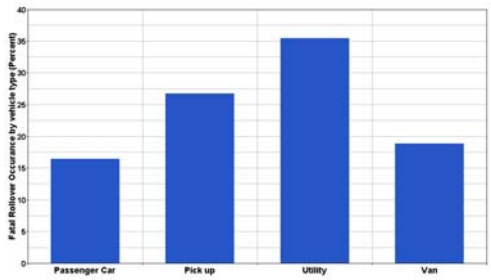

Figure 2. Fatal rollover occurrence by vehicle types.

According to 2001 FARS (Fatality Analysis Reporting System), only eight percent of the vehicles involved in rollover accidents resulted in twenty one percent of the serious injuries and thirty one percent of the fatalities. This makes rollover occupant protection an important research. It mandates a proper understanding of the single loop restraint dynamic behavior during rollover accidents. Several studies were conducted in the past; such as, Arndt et al. [4] conducted a study to correlate restraint slack and occupant excursion. Similarly, Glen Rains et al. [5] demonstrated the influence of a D-ring location on the dummy head excursion using RRT (Rollover Restraint Tester). James F. Pywell et al. [6] demonstrated the effectiveness of a restraint in reducing vertical and lateral head excursion when restraint is integrated with the seat using laboratory test fixture. All these studies are conducted using a laboratory tester with the quasicstatic and dynamic approach. Thorbole et al. [7] in their study demonstrated the effect of gravity on the occupant kinematics when using the laboratory tester compared to the airborne phase of rollovers, when acceleration due to gravity does not result in any relative motion between the vehicle and the occupants.

To address the limitation of a laboratory test to evaluate the performance of different restraints and their configuration, a MADYMO [8] computational model of a full scale rollover test was developed. The objective of this computational study is to compare the head excursion of a far side and near side ATD during the rollover event and to compare the performance of conventional continuous single loop restraints with seat integrated restraints by quantifying the head excursion. This study also quantifies the head excursion with an extra two point restraint added to the three point restraint.

METHODOLOGY

Volvo V70 Remotely Tripped Rollover test

A 2001 Volvo V70 XC, 4-door was used for the full scale trip rollover; as shown in Figure 3.

Figure 3. Test vehicle before rollover.

The vehicle was piloted remotely using a radio control system with the driver in the chase vehicle. The steering servo was capable of providing 11.3 N.m (100in *lbf) of maximum torque. It allowed 4 revolutions at 1000deg/sec maximum. The brake servo allowed 534 N (120 lbf) maximum force, and the throttle allowed 89 N (20lbf). The vehicle was accelerated at full throttle from a complete stop. Prior to approaching the edge of the concrete, a right steer input was initiated followed by a hard left steer input causing the vehicle to yaw counterclockwise and positioning itself approximately parallel to the concrete edge prior to the intended point of trip. The trip mechanism involved a ditch with loose soil 15m (50 feet) long, 0.2m (8 inch) wide and a 0.15m (6 inch) curb height; as shown in Figure 4.

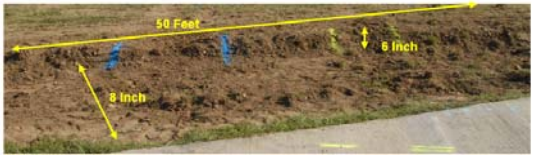

Figure 4. Trip mechanism using lose soil ditch.

The vehicle was instrumented with an IST Motion Master EDR 6DOF stand alone, 6-axis data acquisition system to measure the accelerations and angular rates. The instrument was oriented as per SAE vehicle axis convention and was fixed near the shift stick; as shown in Figure 5.

Figure 5. Instrumentation fixed near shift stick.

Four non-instrumented ATD'S were positioned in the vehicle, two in front and two in the second row; as shown in Figure 6.

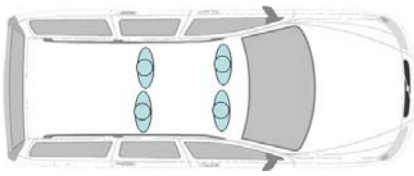

Figure 6. ATD position in the vehicle.

Figure 7 shows linear acceleration data. Figure 8 shows angular velocity data.

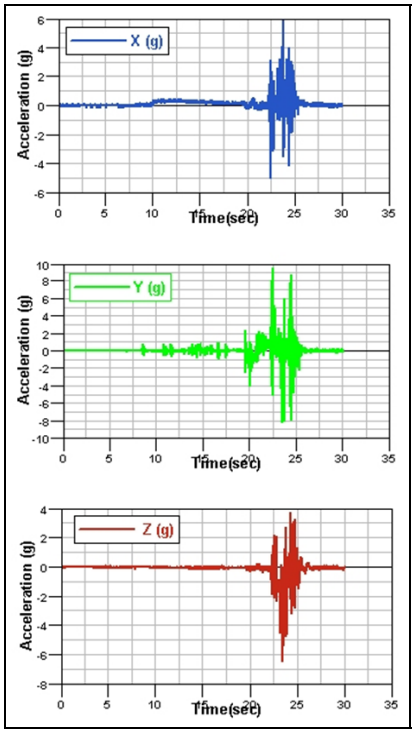

Figure 7. Acceleration data acquired during the test.

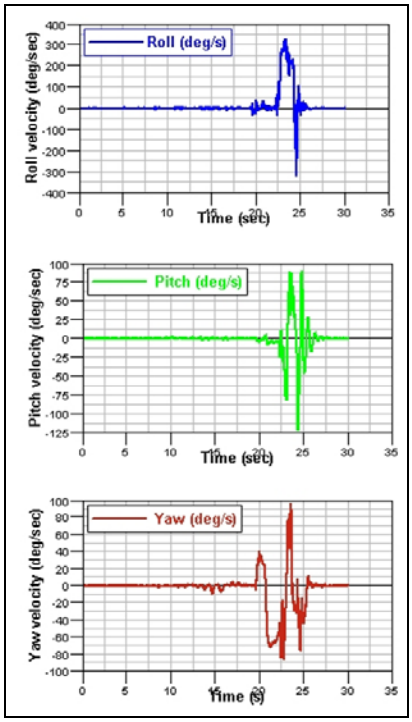

Figure 8. Angular data acquired during the test.

The main intention of this full scale rollover test was to demonstrate the occupant retention capability of modified glazing and door frame. The factory installed tempered glass WSA replaced with laminated glazing with a 7mil clear polyester film applied to the inner surface of the laminated glass. A Hybrid III 5th percentile female dummy was used as a restrained driver with a Hybrid II 50th percentile male dummy as a restrained front passenger. Second row passengers were two unrestrained Hybrid III 5th percentile female dummies. The vehicle motion data acquired during this test was used for the computational analysis intended to evaluate the performance of different restraint in terms of head excursion. Figure 9 shows the rollover sequence from approximately 22.34 sec when the vehicle hit the curb in the ditch. The vehicle rolled once, passenger side leading, without any airborne phase having a 321 deg/sec peak roll velocity. Figure 10 shows the post rollover condition of the vehicle which indicates no failure of the glass except for fractured windshield and back lite.

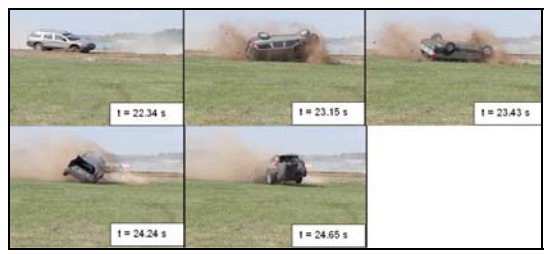

Figure 9. Rollover sequence after vehicle is tripped.

Figure 10. Post rollover vehicle condition.

For the computational analysis the motion data is used from the point where vehicle hits the curb.

Computational Analysis

The biodynamic code MADYMO is used for the kinematic analysis of the front row restrained occupants. This analysis is conducted with the intention of quantifying the front row occupant head excursion with different belt configurations using actual vehicle kinematics as obtained during a full scale rollover test. The data is used from the point where the vehicle hits the curb in

order to reduce the simulation time. MADYMO Version 6.3.1 developed by TASS, running on Intel Quad core Xeon 2.33GHz was used to develop the rollover simulation.

Model Overview - The computational model consists of an ellipsoidal vehicle interior coupled with two Hybrid III 50th percentile male ATD's positioned in the driver and passenger seat. The finite element belt model is used to restrain the occupants. Simulations are conducted for different restraint types to quantify the head excursion.

Interior Geometry - The interior of the vehicle is modeled by measuring the dimensions from the test vehicle. MADYMO ellipsoids are used to create the geometry surface. The interior consists of front seats a second row seat with dash board and steering. Figure 11 shows the modeled interior geometry of the vehicle. The glass is not modeled for this analysis. A free joint is positioned at the location where instrumentation was attached to obtain the vehicle kinematics.

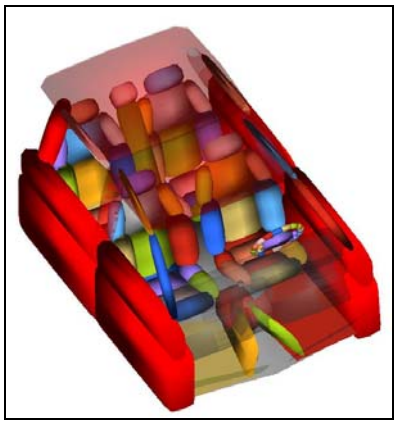

Figure 11. Vehicle interior geometry using ellipsoids.

The standard stiffness characteristics of the seat and the interior are obtained from the application manual of MADYMO [9]. A friction coefficient of 0.2 was used to model contact between occupant and the interior.

Seatbelt – The conventional three-point, single loop belt was modeled, as per location of the D-ring, buckle and floor anchor point in the test vehicle. The D-ring location for the integrated system was assumed on the seat back. The finite element belt in combination with the linear belt segment is modeled to restraint the occupant. The webbing characteristic is obtained from the application manual for MADYMO. A friction coefficient of 0.2 is modeled between the occupant and the belts.

ATD – Hybrid III 50th percentile dummies are used as the driver and the passenger. Initial joint positions of driver's shoulder and elbow are adjusted to replicate steering interaction. No joints in both dummies were locked.

Assembly of Sub-Models – To complete the biodynamic simulation of a rollover accident with different restraints, all of the subsystems as described in the previous section require integration. The ATD's were positioned on the seat and then the restraints were looped around them. The ATD's are allowed to settle down under gravity before they are restrained. Figure 12 shows the complete simulation set up with different restraints.

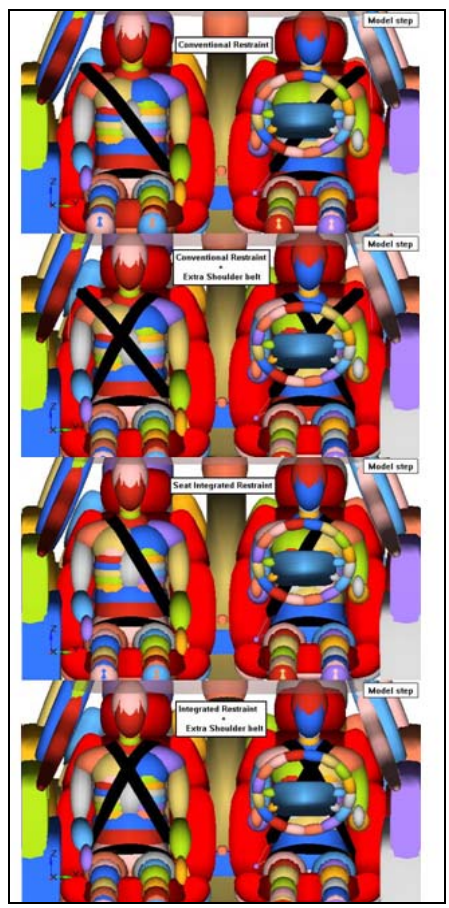

Figure 12. Simulation set up with different restraints.

Response measurement – For each simulation the head excursion of the driver and

the passenger is quantified. This excursion is measured relative to the marker body attached to the vehicle; as shown in the Figure 13. Initially, this marker coincides with the CG of head. The Y displacement provides the lateral excursion relative to this marker, and the Z displacement provides the vertical excursion relative to this marker.

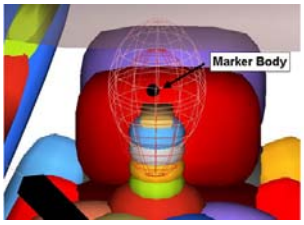

Figure 13. Head excursion measured relative to the marker body.

Simulation time – The actual rollover event was 30 seconds. The simulation motion file is modified to reduce the run time by starting it from the point when the vehicle makes a right turn followed by a hard left turn prior to its trip. The time step used is 10^{-5} with the Euler integration method. The computational time required for this simulation with the FE belt and two dummies was approximately three hours.

RESULTS

The head excursion is quantified relative to the marker body. The head excursion is quantified for two parts of a single rollover event. It is observed that the vehicle completed one roll anticlockwise as seen from the front, followed by additional 40 deg roll, and then fell back on the wheels clockwise in a 40 deg position. The head excursion is reported separately for two phases in a single plot. Figure 14 shows the roll angle of the vehicle with respect to the time and two different phases, as described earlier in this section.

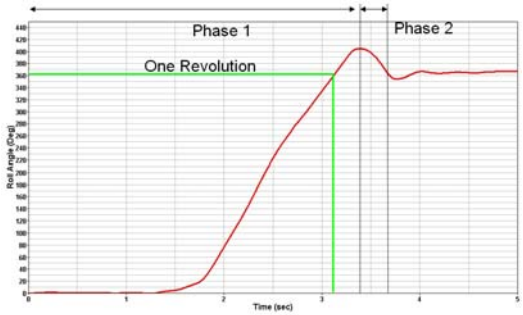

Figure 14. Vehicle roll angle plot during rollover test.

The simulation sequence for each run is reported in the appendix.

Conventional Restraint

Lateral and vertical head excursion is quantified and compared for driver and passenger. Figure 15 shows the lateral head excursion. Figure 16 shows the vertical head excursion for driver and the passenger. The solid blue curve represents the driver, and the dotted red curve represents the passenger. The passenger negative lateral excursion value in the plot is outboard head movement. The driver positive lateral excursion value is an outboard head movement. The positive value of the vertical excursion is an upward movement of the head for both driver and passenger.

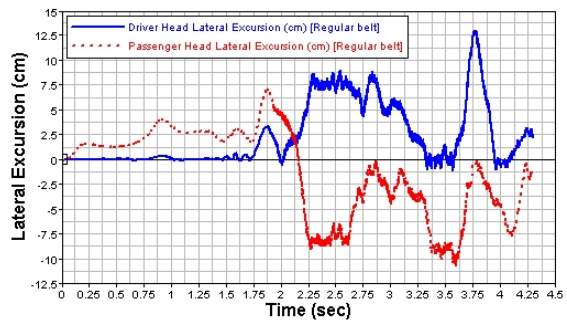

Figure 15. Lateral head excursion for driver and passenger with a conventional belt.

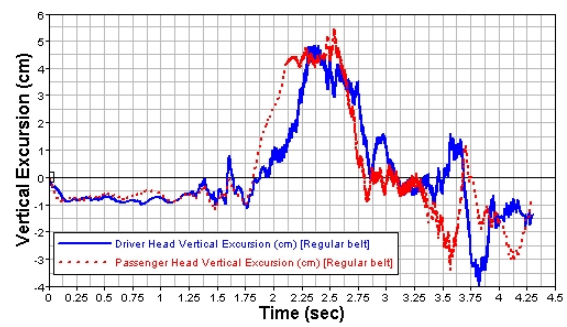

Figure 16. Vertical head excursion for driver and passenger with a conventional belt.

In phase one the peak driver head lateral excursion is 8.57 cm outboard and the passenger head lateral excursion is 8.7 cm. The maximum driver head outboard excursion for phase two is 12.9 cm. The vertical head excursion for driver is 4.7 cm, and 5.25 cm for the passenger. The maximum head lateral excursion occurs in the second phase when the vehicle falls back on the ground after rolling 40 deg about the passenger side. At the peak roll rate the lateral outboard

excursion for the passenger head is 5.2 percent higher than the driver head. The vertical excursion is almost identical. Figure 17 shows the dummy kinematics at peak roll rate.

Figure 17. Driver and passenger kinematics at peak roll rate with conventional restraint.

Seat Integrated Restraint

Figure 18 and Figure 19 show the lateral and vertical head excursion for driver and passenger. The solid blue curve represents the driver and the dotted red curve represents the passenger. The Passenger negative lateral excursion value in the plot is outboard head movement. The driver positive lateral excursion value is an outboard head movement. The positive value of vertical excursion is an upward movement of head for both driver and passenger.

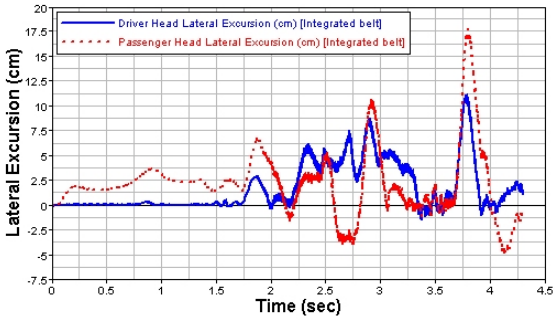

Figure 18. Lateral head excursion for driver and passenger with a seat integrated belt.

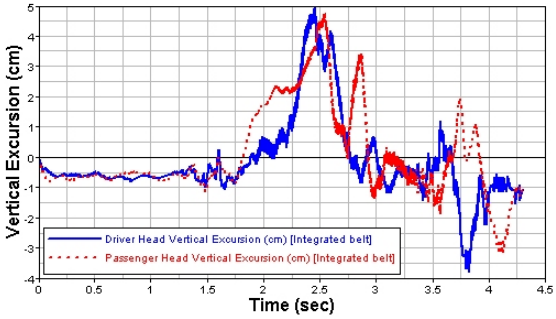

Figure 19. Vertical head excursion for driver and passenger with a seat integrated belt.

The peak driver head lateral excursion in phase one is 8.44 cm outboard and the peak lateral excursion for the passenger is 10.29 cm inboard. Passenger maximum outboard excursion for phase one is 3.46cm. In phase two the passenger head inboard excursion is 17.5 cm and the driver outboard head excursion is 10.8 cm. The peak vertical excursion for the driver in phase one is 4.71 cm, as compared to 5.58 cm for the passenger. At peak roll rate the lateral outboard excursion for the driver head is 5.16 cm and 2.75 cm for the passenger inboards with identical vertical excursion. Figure 20 shows the dummy kinematic at peak roll rate.

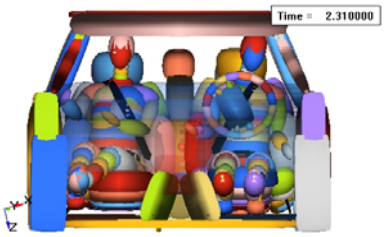

Figure 20. Driver and passenger kinematics at peak roll rate with integrated restraint.

Conventional Restraint Plus Additional Shoulder Belt

In this restraint an additional shoulder harness is added to a conventional restraint, such that the new belt crosses the shoulder belt of the conventional restraint. The top anchor point for the additional belt is on the seat. The bottom anchor point is on the floor. Figure 21 and Figure 22 show the lateral and vertical head excursion for driver and passenger. The solid blue curve represents the driver and the dotted red curve represents the passenger. The sign convention for head excursion is similar, as discussed in the previous section.

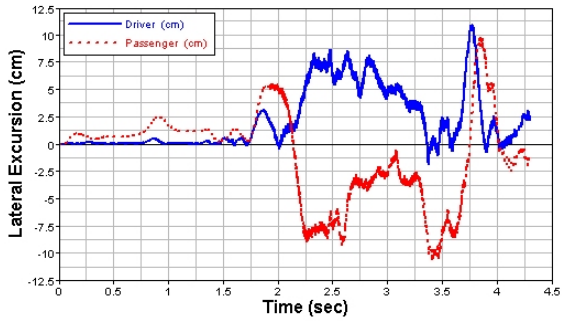

Figure 21. Lateral head excursion for driver and passenger with a five point restraint.

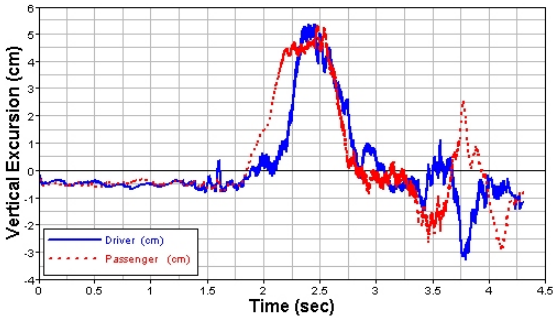

Figure 22. Vertical head excursion for driver and passenger with a five point restraint.

The peak driver lateral excursion in phase one is 8.25 cm outboard and 10.09 cm outboard for the passenger. In the second phase the driver outboard excursion is 10.85 cm and passenger inboard excursion is 9.71cm. The peak vertical excursion for driver and passenger is 5.2 cm in phase one. At peak roll rate the lateral outboard excursion for the passenger head is 23 percent higher than the driver head with similar vertical excursion. Figure 23 shows the dummy kinematic at peak roll rate.

Figure 23. Driver and passenger kinematics at peak roll rate with extra shoulder belt in conventional restraint.

Seat Integrated Restraint Plus Additional Shoulder Belt

In this restraint an additional shoulder harness is added to a seat integrated restraint, such that new belt crosses the shoulder belt of the conventional restraint. The top anchor point for the additional belt is on the seat and the bottom anchor point is on the floor. Figure 24 and Figure 25 show the lateral and vertical head excursion for the driver and the passenger. The solid blue curve represents the driver and the dotted red curve represents the passenger.

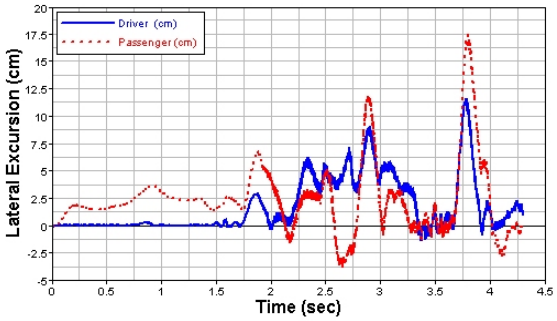

Figure 24. Lateral head excursion for driver and passenger with a five point restraint.

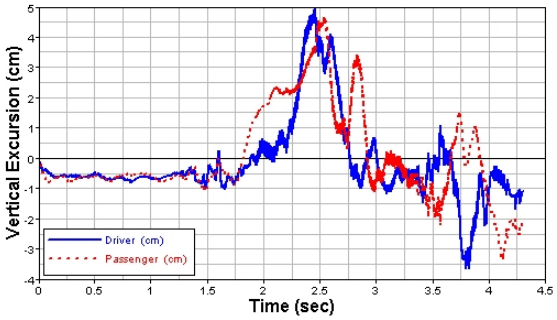

Figure 25. Vertical head excursion for driver and passenger with a five point restraint.

The peak driver lateral excursion in phase one is 8.64 cm outboard and 11.7 cm inboard for the passenger. In the second phase the driver outboard excursion is 11.25 cm and the passenger inboard excursion is 16.9 cm. The peak vertical excursion for driver is 4.8 cm and 4.5 cm for the passenger. At peak roll rate the lateral outboard excursion for the driver head is 4.82 cm and 2.71 cm for the passenger inboards with identical vertical excursion. Figure 26 shows the dummy kinematic at peak roll rate.

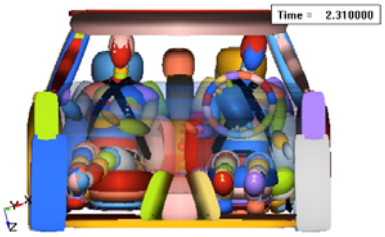

Figure 26. Driver and passenger kinematics at peak roll rate with extra shoulder belt in integrated restraint.

Dynamic Comparison of Different Restraint Types

All the restraint types as described above are compared with each other to identify the dynamic performance of these restraints during this rollover test. The performance is measured in terms of driver and passenger head excursion values. The head excursion is compared at the peak roll rate in phase one, and when the vehicle drops down on its wheels in phase two. Figure 27 shows the comparison of the driver head lateral excursion with different restraint types. This plot clearly indicates 31.4 percent less head outboard excursion for an integrated restraint when compared to a conventional restraint at peak roll velocity. This plot also shows no significant change in lateral outboard excursion with the addition of an extra shoulder strap to a conventional and an integrated restraint. In the second phase integrated restraint results in 15.5 percent less outboard lateral head excursion. Figure 28 shows the driver head vertical excursion comparison which indicates 52.17 percent less vertical excursion with the integrated restraint when compared to the conventional restraint at peak roll rate. This plot also shows no significant change in vertical excursion with addition of an extra shoulder strap to conventional and integrated restraints.

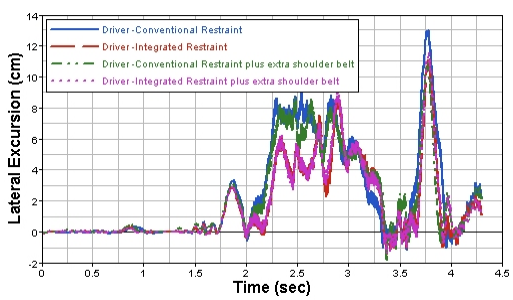

Figure 27. Driver head lateral excursion for different restraints.

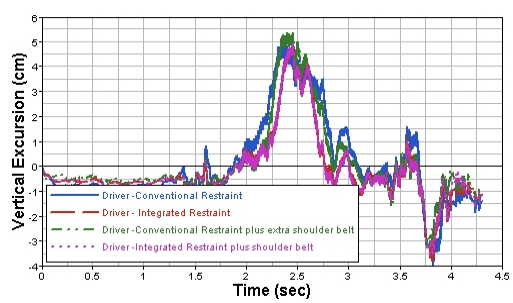

Figure 28. Driver head vertical excursion for different restraints.

Figure 29 shows the lateral head excursion for the passenger which indicates 8.8 cm outboard head lateral excursion for the conventional restraint as compared to 2.8 cm of inboard head excursion with an integrated restraint at peak roll velocity. This plot also indicates that the head stays outboard at a maximum value for 0.25 sec with the conventional restraint. In the second phase the integrated restraint results in 17 cm inboard excursion of the head as compared to 0.4 cm for the conventional restraint. Figure 30 shows the passenger head vertical excursion comparison which indicates 48 percent less vertical excursion with an integrated restraint when compared to the conventional restraint at peak roll rate. This plot also shows no significant change in vertical excursion with the addition of an extra shoulder strap to conventional and integrated restraints.

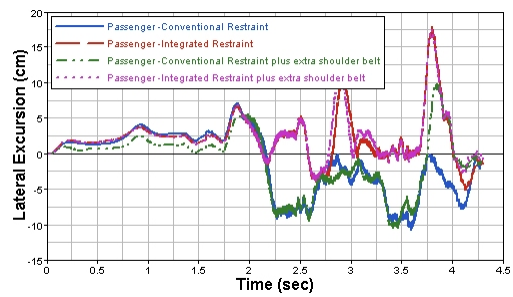

Figure 29. Passenger head lateral excursion for different restraints.

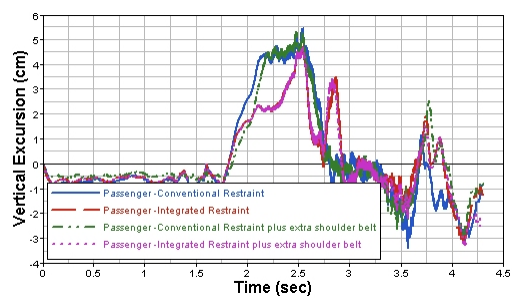

Figure 30. Passenger head vertical excursion for different restraints.

CONCLUSIONS

This study has demonstrated the dynamic comparison of different restraints in terms of head excursion during an actual rollover accident. Front row occupants head lateral and vertical excursions were measured and compared.

The integrated restraint results in less vertical and outboard lateral head excursion as compared

to the conventional restraint at peak roll velocity. As the vehicle start rolling the shoulder belt slip over the shoulder of the driver with the conventional restraint. No slip occurs with the integrated restraint. The addition of an extra shoulder belt to the conventional and integrated restraints does not have any significant effect on the head excursion for this rollover accident. The head excursion of a far side occupant is increased during the second phase of the rollover when the vehicle falls back on the far side wheel.

REFERENCES

[1] Glassbrenner, D. 2003. "Estimating the Lives Saved by Safety Belts and Air Bags." 18th ESV Paper no 500,Nagoya, Japan,May:19-22

[2] Martha,W.B.,Cochran,J.E.,King,D and Burke,D.S. 2007. "Occupant Dynamics in Rollover Crashes:Influence of Roof Deformation and Seat Seat Belt Performance on Probable Spinal Column Injury."Annals of Biomedical Engineering, Vol.35, pp.1973-1988

[3] Traffic Safety Facts, 2005,NHTSA

[4] Arndt,M.W.,Mowry,G.A.,Baray,P.E.and Clark,D.A. "The Development of a method for Determining Effective Slack in Motor Vehicle Restraint System for Rollover Protection." Society of Automotive Engineering, Paper Number 970781

[5] Rains,G.,Elias,J. and Mowry,G. 1998. "Evaluation of Restraints Effectiveness in Simulated Rollover Conditions." ESV Paper no 98-S8-W-34

[6] Pywell,J.F.,Rouhana,S.W.,Mccleary,J.D. and Desaele,K.H.1997. "Characterization of Belt Restraint System in Quasi-static Vehicle Rollover Tests" Society of Automotive Engineering, Paper Number 973334

[7] Thorbole,C.K.,Batzer,S.A. and Renfroe,D.A.2007. "Evaluation of dynamic spit tester using computational biomechanics for occupant ejection mitigation research." 5th IASTED International Conference, Biomechanics, Aug 20-22,Honolulu,Hawaii,USA.

[8] "MADYMO Database Manual, Version 6.3.1", Anon., TNO Road Vehicle Research Institute, Delft, Netherlands

[9] "MADYMO Application Manual, Version 6.3.1", Anon., TNO Road Vehicle Research Institute, Delft, Netherlands

APPENDICES

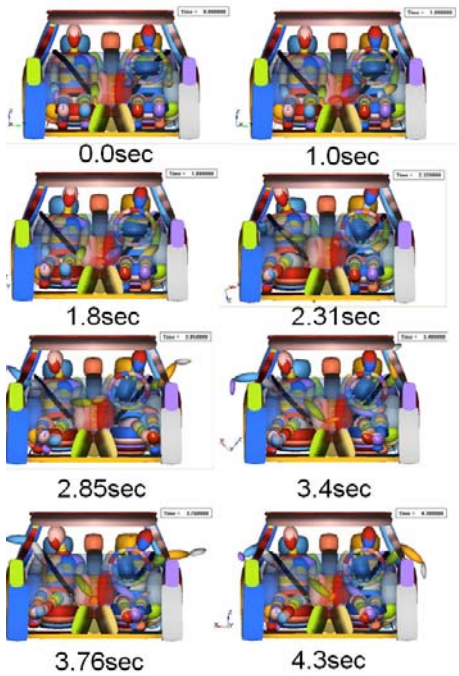

Figure31. Simulation sequence with the conventional restraint.

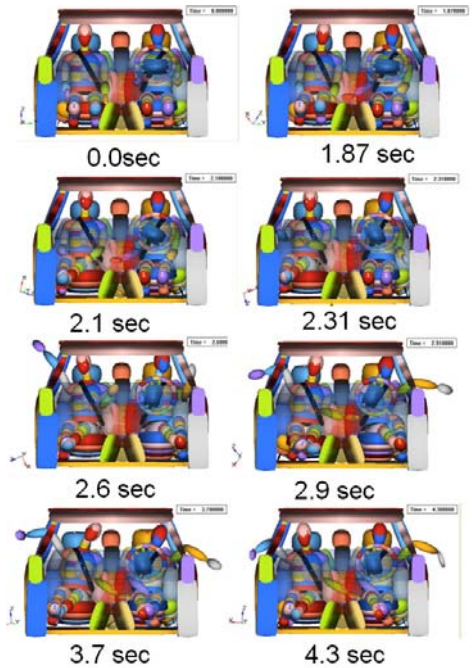

Figure32. Simulation sequence with the integrated restraint.

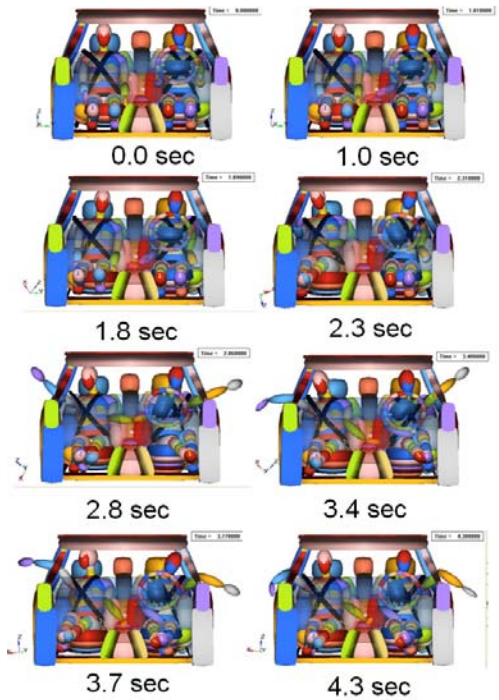

Figure33. Simulation sequence with the conventional restraint plus extra shoulder belt.

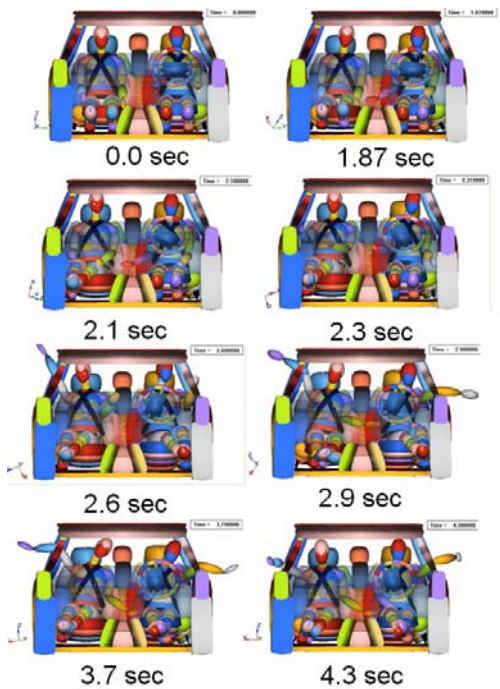

Figure34. Simulation sequence with the integrated restraint plus extra shoulder belt.